Available online at www.sciencedirect.com
ScienceDirect
Bioorganic Chemistry 36 (2008) 33–45
BIOORGANIC CHEMISTRY
www.elsevier.com/locate/bioorg

Cleavage of RNA by an amphiphilic compound lacking traditional catalytic groups

N.A. Kovalev, D.A. Medvedeva, M.A. Zenkova *, V.V. Vlassov

Institute of Chemical Biology and Fundamental Medicine, SB RAS, 8 Lavrentiev Avenue, 630090 Novosibirsk, Russian Federation

Received 7 August 2007
Available online 3 December 2007

Abstract

Recently, in experiments with combinatorial libraries of amphiphilic compounds lacking groups, known as catalysts of transesterification reaction, we discovered novel RNA-cleaving compounds [N. Kovalev, E. Burakova, V. Silnikov, M. Zenkova, V. Vlassov, Bioorg. Chem. 34 (2006) 274–286]. In the present study, we investigate cleavage of RNA by the most active representative of these libraries, compound named Dp12. Sequence-specificity of RNA cleavage and influence of reaction conditions on cleavage rate suggested that Dp12 enormously accelerates spontaneous RNA cleavage. Light scattering experiments revealed that the RNA cleavage proceeds within multiplexes formed by assembles of RNA and Dp12 molecules, at Dp12 concentration far below critical concentration of micelle formation. Under these conditions, Dp12 is presented in the solution as individual molecules, but addition of RNA to this solution triggers formation of the multiplexes. The obtained data suggest a possible mechanism of RNA cleavage, which includes interaction of the compound with RNA sugar-phosphate backbone resulting in changing of ribose conformation. This leads to juxtaposition of the 2′-hydroxyl group and internucleotide phosphorus atom at a distance needed for the transesterification to occur.

Keywords: RNA cleavage; Artificial ribonucleases; Conformation effect; Hydrophobic effect; In-line conformation

1. Introduction

Artificial ribonucleases, synthetic compounds capable to catalyze RNA cleavage — can find important applications in molecular biology and biotechnology. A number of artificial ribonucleases capable of cleaving RNA under physiological conditions have been designed [2–19]. Most of them are built of two parts: one, which provides catalyses of transesterification and another one, which provides affinity of the compound to RNA, thus increasing local concentration of a catalyst in the vicinity of linkages to be cleaved. Catalytic part of artificial RNases (here and after aRNases) usually contains complexes of transition metals (Zn^{2+} [2–4], Eu^{3+} [5,6], Pb^{2+} [7,8]) or organic structures bearing functionalities, known to be involved in the catalysis in the active centers of natural ribonucleases (imidazole [9,10], guanidinium, amino or carboxyl groups [11,12]). RNA-binding part of aRNases is built of cationic structures [10, 13–15], intercalating molecules [9,13,16] or antisence oligonucleotides [17–19]. The most active aRNases appeared to be the ones built of metal complexes, however recently non-metal aRNases were synthesized, which display activity comparable to that of the metal complexes [14]. These artificial ribonucleases are conjugates of 1,4-diazabicyclo [2.2.2] octane (DABCO), substituted by an aliphatic fragment at the bridge nitrogen atom and conjugated with imidazole containing structures [10,14]. In experiments with different modified DABCO-based compounds, it was found, that some truncated compounds lacking imidazole residue exhibited considerable ribonuclease activity. These compounds were built of hydrophobic and cationic structures. In experiments with combinatorial libraries of these compounds [1], we identified several efficient RNA-cleaving molecules. The most active of them (Dp12) is built of two diazabicyclo [2.2.2] octane residues,

* Corresponding author. Fax: +7 383 3333677.
E-mail address: marzen@niboch.nsc.ru (M.A. Zenkova).

0045-2068/$ - see front matter © 2007 Elsevier Inc. All rights reserved.
doi:10.1016/j.bioorg.2007.10.003

substituted with tetradecamethylene fragment, and connected by a rigid linker. This was a surprising finding, because the molecule does not contain groups known to participate directly in the transesterification reaction. There is no clear understanding how cationic and hydrophobic fragments conjugated together could cleave RNA. This finding indicated that hydrophobic domain possesses some features needed for the catalysis of transesterification reaction. It is known, that in general in RNA–protein complexes [20,21] and in natural ribonucleases [22–24] hydrophobic interactions play important roles, particularly, in changing conformation of RNA and e.g., in the case of RNases helping the linkage to be cleaved to adopt the most favorable conformation for transesterification [25].

In the present article we describe properties and RNA cleavage by the compound Dp12, identified as the most active among. Results of the study suggest, that this compound cleaves RNA via interactions with its sugar-phosphate backbone, that induce conformational alteration of RNA structure, favorable for transesterification to occur. We have found, that Dp12 enormously enhances rate of spontaneously RNA cleavage and efficiency of catalysis can be considerably increased by synergetic action of Dp12 and OH^-, or imidazole, or monovalent ions.

2. Materials and methods

2.1. Miscellaneous chemicals, enzymes, and RNAs

Chemicals for synthesis were purchased from Aldrich (USA). Chemicals for electrophoresis were purchased from Sigma (USA), [γ-^{32}P]-ATP was from Biosan (Russia). Solutions for RNA handling were prepared using Milli-Q water, filtered through membranes with 0.2 μm pore size (Millipore, USA) and autoclaved. T4 polynucleotide kinase was from Fermentas (Lithuania), ribonuclease T1, bovine alkaline phosphatase were from Sigma (USA). Oligonucleotide r(UCGAAUUUCCACAGAAUUCGU) (ON21) was synthesized by Dr. M. Repkova, (this institute) by standard phosphoramidite chemistry and purified using RP-HPLC.

Transcripts of yeast tRNA^{Phe}, fragments of MDR1 mRNA (190-mer and 670-mer) and fragment of HIV1 RNA (96-mer) were synthesized *in vitro* using linearized plasmids from ICBFM collection: dYF90 (*Bst2UI*), pBluescriptMDR670 (DraI, Sma1 for 190-mer, and 668-mer, respectively), pHIV2 (FokI), respectively, and T7 RNA polymerase as described earlier [26]. Total tRNA from *Escherichia coli*, used as a carrier to supplement labeled RNAs, was from Vector, Russia.

Dp12 was synthesized by Ms E. Burakova (this institute) as described recently [1].

2.2. Critical micelle concentration of Dp12

Critical micelle concentration (CMC) of Dp12 was determined in Tris–HCl buffer at pH 7.0, containing 0.2 M KCl, 0.1 mM EDTA by static light scattering using a VA Instruments Co., Ltd. LS-01 apparatus (Saint-Petersburg, Russia) calibrated with a dust-free benzene ($R_{90} = 11.84 \times 10^{-6}\text{cm}^{-1}$). The intensity of light scattering (I_{90}) was measured using the vertically polarized light (633 nm) at angle $\theta = 90°$. The CMC was determined by the linear least-squares fitting of the light scattering intensity ratio (I_{90}/I_0) that is the intensity of light scattering normalized to the intensity of the incident light. A sharp increase in the intensity ratio is observed upon a micelle formation.

2.3. Kinetics of the RNA/Dp12 interactions

The kinetics of the RNA/Dp12 interaction was studied by measuring static light scattering of RNA/Dp12 solution. Because the light scattering intensity ratio (I_{90}/I_0) is directly proportional to the molecular mass and size of particles present in solution, the changes of the intensity of light scattering (I_{90}) versus time were measured at angle $\theta = 90°$.

The weighted average molecular mass, M_w, the radius of gyration, R_G, and the second virial coefficient, A_2, of the complexes Dp12 with RNA (96-mer and 668-mer) were determined by laser multiangle static light-scattering in a Tris–HCl buffer at pH 7.0, containing 0.2 M KCl, 0.1 mM EDTA, Dp12 at concentration 1×10^{-5} M, and RNA (96-mer or 668-mer) at concentration 0.1 mg/ml. The Rayleigh ratio R_θ was measured using the vertically polarized light (633 nm) at angles in the range $40° \leqslant \theta \leqslant 140°$ (13 angles) using a VA Instruments Co., Ltd. LS-01 apparatus calibrated as described above. The data were used to plot the angular and concentration dependencies of the ratio $HC/\Delta R_\theta$ according to the Zimm method [27]. Here, C is the particle concentration (g mL^{-1}), ΔR_θ is the excess light scattering over that of the solvent at angle θ, and H is an instrumental optical constant equal to $4\pi^2 n^2 v^2 / N_A \lambda^4$, where N_A is the Avogadro's number, λ is the wavelength of incident light in vacuum, n is the refractive index of the solvent, and v is the refractive index increment of the protein. Values of the weight-average molar mass, M_w, were estimated as averages from the intercepts of both the concentration dependence of $HC/\Delta R_\theta$ as $\theta \to 0$ (the extrapolation was performed on 13 angles) and the angular dependence of $HC/\Delta R_\theta$ as $C \to 0$ (the extrapolation was performed on 5–8 concentrations by dilution of standard reaction mixture by a factor of 1.1–1.5). Values of the radius of gyration, R_G, were estimated from the slope of the angular dependence of $HC/\Delta R_\theta$ as $C \to 0$. Values of the second virial coefficient, A_{pr-pr}, were estimated from the slope of the concentration dependence of $HC/\Delta R_\theta$ as $\theta \to 0$. The second virial coefficient characterizes primarily the thermodynamic affinity of the particles (complexes Dp12 with RNA) to the solvent (a Tris–HCl buffer in our case): it is poor, if $A_{pr-pr} < 0$, or, by contrast, it is good if $A_{pr-pr} > 0$, and it is ideal if $A_{pr-pr} = 0$) [28], i.e. provide the circumstantial evidence for the complexes surface hydrophilicity/hydrophobicity.

The values of M_w, A_{pr-pr}, and R_G presented in this work are averaged data for at least two repetitions of each of the experiments. The experimental error in the determinations of M_w and A_{pr-pr} was estimated as ±10%. The error of the R_G determination was ±5%.

Values of the refractive index increments for the complexes Dp12 with RNA (96-mer and 668-mer) were determined at 635 nm and 37 °C using Shimadzu differential refractometer. The experimental error is ±10%. For complexes Dp12 with RNA (96-mer and 668-mer) these values were unchanged within experimental error in the presence of the RNA studied: $v = 0.32 \times 10^{-3}$ m^3 kg^{-1}.

Values of the hydrodynamic radius R_h of both complexes at different concentrations were estimated in Tris–HCl buffer, at pH 7.0 (0.2 M KCl, 0.1 mM EDTA) by dynamic light scattering [29,30]. The time correlation function of the scattering intensity was measured at 90° with the vertically polarized light (633 nm). The values of the hydrodynamic radius R_h presented in this work are averaged data for ten repetitions of each of the measurements. The error in the R_h determination was ±10%. To determine the hydrodynamic radius from the time correlation function, a special program was used (DYNALS Release 1.5, all rights reserved by A. Golding and N. Sidorenko, VA Instruments Co. Ltd. (Saint Petersburg, Russia)). Temperature during the light-scattering experiments was set constant at 37 °C.

2.4. End labeling of RNAs

5′-End ^{32}P labeling of RNAs were performed as described [31]. Prior to the labeling, RNAs (*in vitro* transcripts) were dephosphorylated using bovine alkaline phosphatase. Labeling of the transcripts was performed with [γ-^{32}P]ATP and T4 polynucleotide kinase [32]. After labeling, RNAs were purified by electrophoresis in 8% denaturing polyacrylamide gel. The labeled RNAs were eluted from the gel by three portions (300 μl each) of 0.5 M ammonium acetate, containing 0.5 mM EDTA and 0.1% SDS, and precipitated with ethanol. RNA pellet was centrifuged, rinsed twice with 80% ethanol, dissolved in water and stored at −20 °C.

2.5. Cleavage experiments

5′-End labeled ON21 was diluted with unlabeled ON21 to final concentration of 5 μM. In the case of transcripts, 5′-end labeled yeast tRNA^{Phe}, a fragment of MDR 1 mRNA and a fragment of HIV 1 mRNA, the reaction mixture were supplied with RNA carrier (total tRNA from *E. coli*) at final concentration of 100 μg/ml. Kinetic and concentration experiments were carried under standard reaction conditions. Standard reaction mixture (10 μl) contained 50,000–100,000 Cherenkov cpm of [5′-^{32}P]-RNA substrate (stabilized by 5 μM ON21 or 100 μg/ml RNA carrier) and 1–1000 μM of the compound Dp12 in 50 mM Tris–HCl buffer, pH 7.0, 0.2 M KCl and 0.5 mM EDTA. In other experiments one or more parameters were varied to assay the influence of reaction conditions.

2.5.1. pH profile assay conditions

pH dependence was investigated within pH range from 5.0 to 8.0: in sodium acetate (pH 5.0–6.2), cacodylate (pH 6.2–7.0) or Tris–HCl (pH 7.0–8.0) buffers. Reaction mixture (10 μl) contained 50,000–100,000 Cherenkov cpm of [5′-^{32}P]-ON21 (stabilized by 5×10^{-6} M ON21) and 10 μM of the compound Dp12 in 50 mM respective buffer, containing 0.2 M KCl, 0.5 mM EDTA. Dp12 activity at the overlapping pH points was compared and the united pH profile was plotted.

After the obtaining data on extents of RNA cleavage at different pH, k_{obs} were calculated as described in [33] according to the following equation:

$$[P]_t = [P]_\infty \times (1 - e^{-k_{obs} \times t}),$$

where $[P]_t$ and $[P]_\infty$ are the extents of RNA cleavage at time t and infinite time (t_∞). We took $[P]_\infty$ equal to 100% as quantitative cleavage of any phosphodiester bond can be achieved.

2.5.2. Buffers influence assay conditions

Cleaving activity of Dp12 in 50 mM buffers (HEPES, MES, Tris, acetate, cacodylate and phosphate) was studied and compared. Reaction mixture (10 μl) contained 50,000–100,000 Cherenkov cpm of [5′-^{32}P]-ON21 (stabilized by 5×10^{-6} M ON21) and 10 μM of the compound Dp12 in 50 mM buffer, containing 0.2 M KCl, 0.5 mM EDTA. For comparison, the highest activity of Dp12 was taken as 100%.

2.5.3. Imidazole stimulation assay conditions

Imidazole concentration dependence was investigated at imidazole concentrations 1, 5, 10, 15, 20, 50 mM. Reaction mixture (10 μl) contained 50,000–100,000 Cherenkov cpm of [5′-^{32}P]-ON21 (stabilized by 5×10^{-6} M ON21), 10 μM of the compound Dp12, 50 mM buffer Tris–HCl, imidazole at the indicated concentration, 0.2 M KCl and 0.5 mM EDTA.

2.5.4. Effect of monovalent ions assay conditions

Activity of Dp12 in the presence of different monovalent cations was studied by replacing K^+ with Li^+, Na^+, Cs^+, or NH_4^+, and concentration of monovalent cations was set at 0, 10, 25, 50, 100, 200, 400 mM. Reaction mixture (10 μl) contained 50,000–100,000 Cherenkov cpm of [5′-^{32}P]-ON21 (stabilized by 5×10^{-6} M ON21) and 10 μM of the compound Dp12 in 50 mM buffer Tris–HCl, one of monovalent cations at the indicated concentration and 0.5 mM EDTA.

Reaction mixtures were incubated at 37 °C for different times (from 1 to 100 hours), reactions were quenched by RNA precipitation with 100 μl of 2% lithium perchlorate in acetone. The RNA pellet was collected by centrifugation and dissolved in the loading buffer (7 M urea and leading

dyes: 0.01% xylene cyanol, 0.01% bromophenol blue). The cleavage products were analyzed in 8% or 15% PAAG containing 8 M urea and TBE × 1 as running buffer. The cleavage sites were assigned by comparison of the electrophoretic mobilities of cleavage products with products of RNA cleavage with RNase T1 and in 2 M imidazole buffer (pH 7.0). Quantitative data were obtained using Molecular Imager FX (Bio-Rad, USA).

3. Results

3.1. Design of artificial ribonuclease and RNA targets

Compound Dp12, built of two positively charged diazabicyclo[2.2.2]octane residues (here and after DABCO, D), substituted at the bridge position with dodecamethylene fragment (12), and connected by a rigid linker—benzene (Fig. 1a) was the most active among tested combinatorial libraries [1]. Substituted DABCO residues were attached to the benzene ring at the *para*-position (p). It was shown [10], that neither DABCO, no tetradecene, no mixture of both possess any RNA-cleavage activity.

Ribonuclease activity of the compound Dp12 was assayed in experiments with synthetic hairpin oligonucleotide ON21 (Fig. 1b) This oligonucleotide folds in a hairpin, containing 7-member loop UCCACAG, which corresponds to nucleotides 60–66 of yeast $tRNA^{Phe}$ known to be particularly sensitive to different cleaving agents [14]. The other RNA substrates prepared by *in vitro* transcription were yeast $tRNA^{Phe}$, 96-mer fragment of HIV1 RNA (Fig. 1c and d), 190- and 668-mer fragments of MDR1 gene mRNA (here and after RNA76, RNA96, RNA190, and RNA668, respectively) [34].

3.2. RNA-cleaving activity of Dp12

Dp12 RNA-cleaving activity was assayed using 5′-labeled oligonucleotide ON21 incubated in Tris–HCl buffer (pH 7.0) at 37 °C at Dp12 concentrations ranged from 1 μM to 1 mM. As it is seen in Fig. 2, Dp12-catalyzed cleavage reaction displays bell-shaped concentration

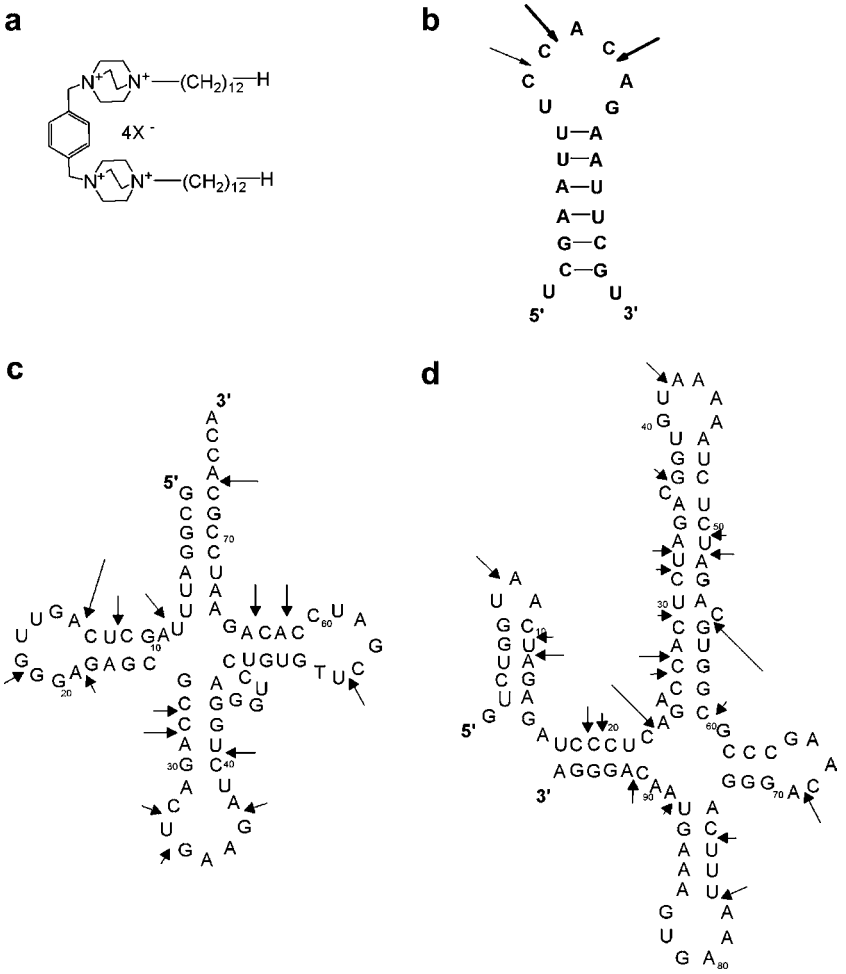

Fig. 1. Structure of artificial ribonuclease Dp12 (a) and RNA substrates used in the experiments: 21-mer oligoribonucleotide (b), yeast $tRNA^{Phe}$ (c) 96-mer fragment of HIV1 RNA (d). Arrows show the sites of cleavages induced by the chemical ribonuclease. Arrow size corresponds to the cleavage intensity.

dependence with the maximum at 10 μM. Similar bell-shaped concentration dependencies of RNA cleavage were observed for the DABCO-based artificial ribonucleases (ABLkCm), bearing tetradecamethylene fragment [14]. Therefore all RNA cleavage experiments with Dp12 were carried out at this concentration. Under condition used the concentration of ON21 was 5 μM, which corresponds to the concentration of phosphates about 0.1 mM. Thus at optimal Dp12 concentration ([Dp12]<<[RNA] (phosphates)) multiple turnover took place. The same maximum (10 μM) of Dp12 concentration profile was observed for other tested RNA targets (yeast $tRNA^{Phe}$, RNA96, and RNA190).

Kinetics of Dp12-catalyzed RNA cleavage were studied in experiments with [5′-^{32}P]-ON21 under standard reaction conditions. As shown in Fig 2b, kinetic curve has typical shape with tendency to saturation and halflife time of ON21 was estimated to be 8 h. Effective rate constant k_{obs} of ON21 cleavage by Dp12 was measured to be 4×10^{-6} s^{-1}, while effective rate constant of RNA self-cleavage at the most labile bonds in ON21 was at least two orders of magnitude lower (primary data not shown).

3.3. Light scattering experiments

The maximal cleavage activity of Dp12 is observed at concentration 10 μM (Fig. 2). Dp12 is an amphiphilic compound, so it should be assayed, in which form it displays cleavage activity: in the form of individual compounds or in the form of micelles. To answer this question the critical micelle concentration (CMC) for compound Dp12 was determined (Fig. 3a) in Tris–HCl buffer (pH 7.0, 0.2 M KCl, 0.1 mM EDTA, at 37 °C). The critical micelle concentration of Dp12 lies at the intersection of lines representing the concentration-dependence of the the normalized scattering intensity at the scattering angle $\Theta = 90°$ that is given by I_{90}/I_0, where I_0 is the primary beam intensity and I_{90} is the corresponding scattering intensity at the scattering

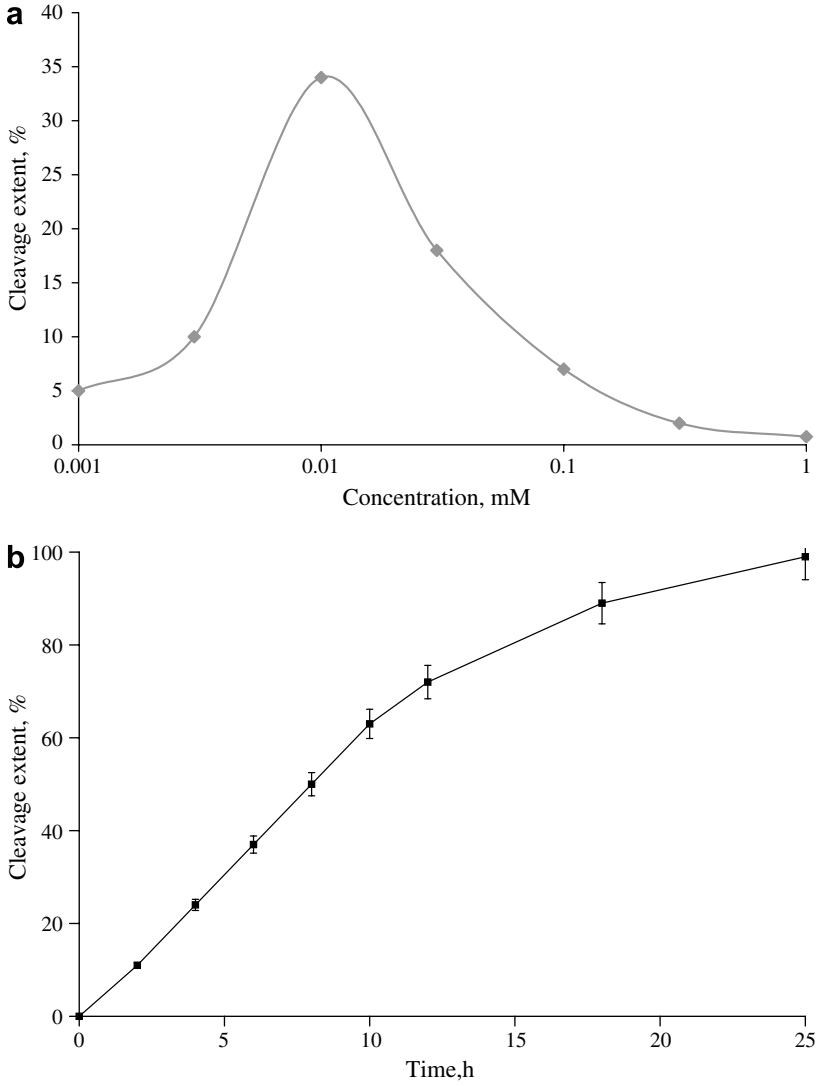

Fig. 2. RNA cleavage by Dp12 under standard reaction conditions (see Section 2). (a) Dp12 concentration profile of ON21 cleavage (incubation time 4 h). (b) Kinetics of [5′-^{32}P]-ON21 cleavage by Dp12 (10 μM).

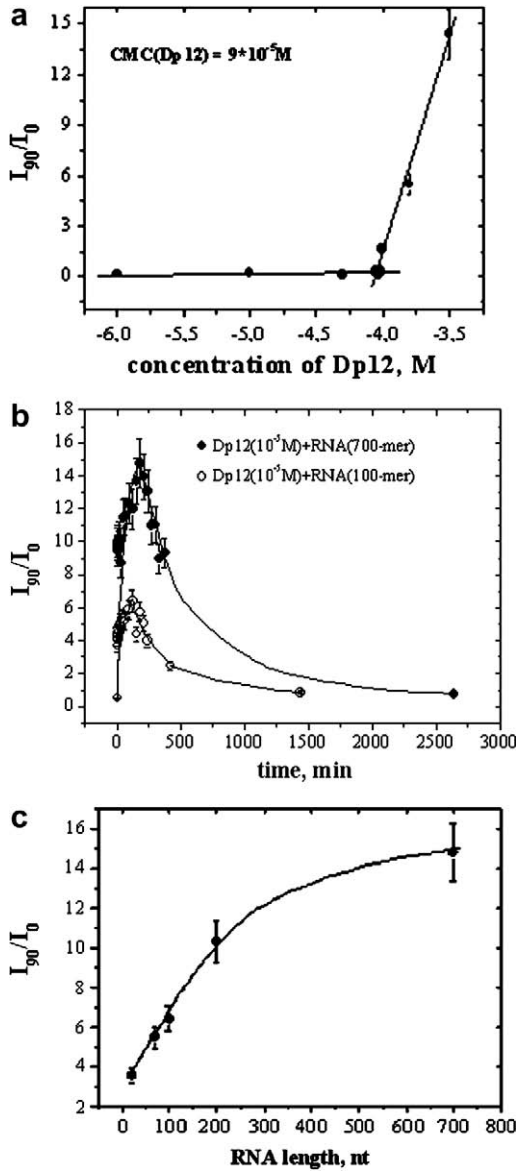

Fig. 3. Results of light scattering experiments (a) The dependence of the light scattering intensity ratio (LSIR) on the logarithm of concentration of Dp12 in Tris–HCl buffer (0, 2 M KCl, 0,1 mM EDTA) at pH 7.0 and 37 °C. (b) The changes in the LSIR for the system Tris–HCl buffer pH 7.0 containing 10 μM Dp12 and 0.1 mg/ml of the RNA substrate (96-mer—open circles and 668-mer—filled circles) at 37 °C. The I_{90}/I_0 value at the start time point (0 min) is the LSIR for the Dp12 solution prior to the RNA adding. (c) The dependence of the maximum values of LSIR versus RNA length in standard reaction conditions with 10 μM Dp12 and 0.1 mg/ml of the RNA substrates (21-mer, 76-mer, 96-mer, 190-mer, and 668-mer) at 37 °C.

angle $\Theta = 90°$. One of the lines represents the intensity of light scattering from individual molecules of Dp12 at low Dp12 concentrations and another line corresponds to increasing additional contribution of the micelles of Dp12 to the overall intensity of light scattering (Fig. 3a). We found that the CMC of Dp12 is equal to 90 μM. Thus Dp12 displays maximal cleavage activity far below CMC.

To understand how Dp12 cleave RNA, interaction of the compound with RNA was assayed using the method of static light scattering. Fig. 3b and c display time dependencies of light scattering intensity ratio (LSIR, I_{90}/I_0) of Dp12 solution (10 μM) after addition of RNA substrates (RNA96 and RNA668) and dependencies of light scattering intensity ratio of Dp12/RNA solution on the length of RNA substrates, respectively. As shown in Fig. 3b, at the initial stage of the interaction LSIR distinctly increases, up to the maximum achieved after 120–180 min of incubation, and then LSIR decreases to the initial value. As shown in Fig. 3c, weight-average molar weight and size of complexes increase nonlinearly with the increasing of RNA fragment length. The time required for decreasing LSIR to the initial value correlate well with the kinetics of decreasing of RNA size as the result of its cleavage (primary data not shown).

To characterize the molecular complexes formed by Dp12 and RNA, weight-average molecular weight (M_w), hydrodynamic radius (R_h), gyration radius(R_G), and second virial coefficient A_2 for complexes Dp12/RNA (RNA96 or RNA668) were calculated by the methods of static and dynamic light scattering (see Section 2). The calculated data are shown in Table 1. It is seen that the parameter I_{90}/I_0 is in direct proportion to weighted average molar weight and the size of complexes formed, while ratio value $\rho = R_G/R_h < 0.7$–1 indicates that in solution of RNA/Dp12 multimeric complexes (multiplexes) are formed [29]. Comparison of coefficients A_2 suggested that complex of Dp12 with 96-mer RNA have hydrophobic surface ($A_2 < 0$), while complex of Dp12 with 668-mer RNA have hydrophilic surface ($A_2 > 0$). Difference of the complexes affinity to solvent could be possibly explained by different charge ratio Dp12 (+)/RNA (−). In the case of RNA96, at the concentrations used, negative charges of RNA are mostly neutralized by positive charges of Dp12 molecules and surface of such complexes become hydrophobic, while in the case of RNA668, negative charges are only partly compensated, so the surface of complex is hydrophilic.

3.4. Sequence-specificity of RNA cleavage by compound Dp12

Sequence-specificity of RNA cleavage by the compound Dp12 was investigated in experiments with three different RNAs: yeast $tRNA^{Phe}$, RNA96 and RNA190 (data are summarized in Fig. 1b–d). Cleavage of RNA occurs in a nonrandom manner: in general the major cleavage sites are phosphodiester bonds in Pyr—A motifs. Pyr—C and C—N motifs (N-any nucleotide) are cleaved less efficiently and N—G motifs are cleaved considerably slower. Pyr—A phosphodiester bonds located in the loops display the highest sensitivity towards cleavage. These are bonds C_{10}—A_{11}, C_{12}—A_{13} in ON21, C_{13}—A_{14} in $tRNA^{Phe}$ and U_7—A_8, C_{22}—A_{23}, U_{41}—A_{42}, C_{69}—A_{70} in RNA96 (Fig. 1c). Some strong cuts occur in the junctions (U_8—A_9 in $tRNA^{Phe}$ and C_{72}—A_{73} in RNA96). Phosphodiester bonds located in the double-stranded RNA regions are cleaved consider-

Table 1
Molecular and thermodynamic parameters of the complexes formed as a result of interactions of the Dp12 with RNA (100-mer and 700-mer) in a Tris–HCl buffer at 37 °C (pH 7.0, 0.2 M KCl, 0.1 mM EDTA)

Sample	$M_w \times 10^6$ (Da)	$A_2 \times 10^5$ (m^3 mol kg^{-2})	R_G (nm)	R_h (nm)	R_G/R_h
Dp12(10^{-5} M) + RNA(100-mer)	143.5	−1.2	197	300	0.65
Dp12(10^{-5} M) + RNA(700-mer)	310.96	2.19	134	300	0.45

The experimental error in the determinations of M_w, A_2 and R_h was estimated as ±10%. The error in the R_G determination was ±5%.

ably less efficiently and these cuts appeared after longer incubation.

In some cases cleavage of Pyr—C motifs is observed but with a low efficiency. For example these are C_9—C_{10} linkage in ON21, U_{55}—C_{56} in $tRNA^{Phe}$, U_{51}—C_{52} and C_{44}—C_{45} — in the double-stranded region of RNA190 (primary data not shown).

C-G and C-U bonds are cleaved within some structures, apparently due to the folding providing a conformation favoring the transesterification to occur, e.g., C_{55}—G_{56} bond located in a one base bulge-loop (RNA96) and C_{18}—U_{19} bond adjacent to G—U base pair closing the stem (RNA190). Cleavage within some of D-G motives (D = A, G, U) located in single-stranded regions is observed, although with very low efficiency.

3.5. Effect of cleavage conditions

The influence of cleavage conditions on the catalytic activity displayed by Dp12 was assayed in experiments with

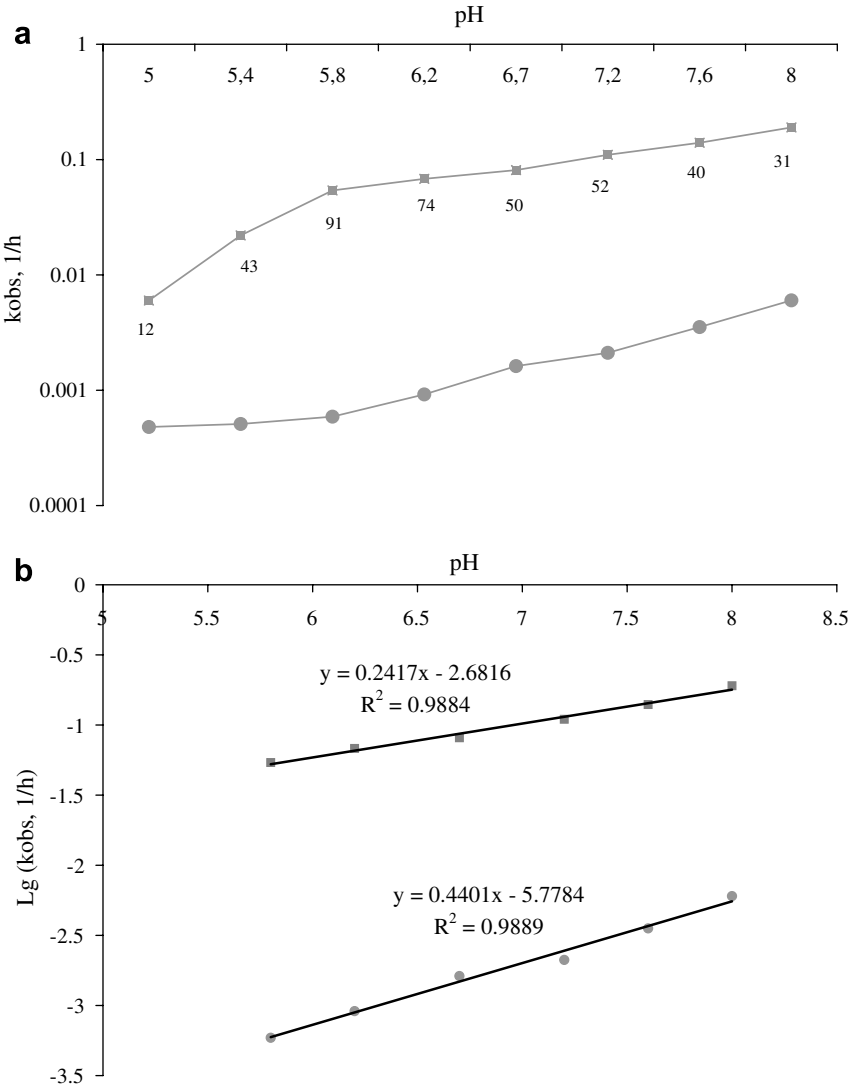

Fig. 4. (a) profile of RNA self-cleavage (k_{obs}^{self}, circles) and RNA cleavage by Dp12 (k_{obs}^{cat}, squares) in logarithmic scale. Numbers below the k_{obs}^{cat} graphic are ratio $k_{obs}^{cat}/k_{obs}^{self}$. (b) Slopes of linear curves for log k_{obs} versus pH diagrams. Reaction conditions: 5 μM ON21, 10 μM Dp12, 50 mM buffer, pH 5.0–8.0, 0.2 M KCl, 0.1 mM EDTA, 37 °C, 12 h.

ON21. In these experiments type and pH of buffer, stimulation of the reaction by imidazole and effect of monovalent cation type and concentration were studied.

pH profile was measured within the pH interval from 5.4 to 8.0 in three buffers: NaAc–HAc (pH 5.0–6.2), potassium cacodylate–KOH (pH 6.2–7.0), Tris–HCl (pH 7.0–8.0). ON21 was incubated in the absence or in the presence of Dp12 (10 μM) in the appropriate buffer and extent of ON21 cleavage was measured. For every pair of buffers with overlapping pH, the data corresponding to the equal pH values, were selected to plot the united graph. k_{obs} calculated both for the catalyzed and for the self-cleavage reactions are plotted in Fig. 4a. It is seen, that in the case of the non-catalyzed reaction, substantial increase of k_{obs} is observed at pH above 6.2 with sharp increase of k_{obs} at pH 8.0. In the case of Dp12-catalyzed cleavage, linear dependence of k_{obs} versus pH is observed within pH range 5.0–7.6, and similar sharp increase of k_{obs} at pH 8.0 is observed. This increase of the rate of RNA cleavage at alkaline pH is in accordance with the mechanism of RNA cleavage including activation of 2′-OH groups of RNA. Dp12 strongly enhances the rate of phosphodiester bonds cleavage at all tested pH, especially below 7.0: at pH interval 5.4–7.2 ratio $k_{obs}^{cat}/k_{obs}^{self}$ is over 90, while at pH over 7.2 this ratio decreases up to 30 at pH 8.0. It looks like at alkaline pH with increasing concentration of OH^- role of catalysis is diminished. The dependences of log k_{obs} both for catalyzed and for self-cleavage reactions versus pH are plotted in Fig. 4b.

It was shown earlier [35], that imidazole accelerates RNA cleavage by some aRNases. The imidazole stimulation profile of ON21 cleavage by Dp12 (Fig. 5) is a bell-shaped curve with the maximal cleavage activity of Dp12 observed at 10 mM imidazole. Increasing of imidazole concentration above 10 mM, resulted in decreasing of RNA cleavage by Dp12. At optimal imidazole concentration (10 mM) 2.5-fold enhancement of cleavage efficiency of ON21 was achieved.

Stimulation of the reaction at low concentrations of imidazole could be possibly explained by binding of imidazole molecules to phosphates, followed by well-known intramolecular transesterification reaction: the 2′-OH groups deprotonation and consecutive attack of the deprotonated hydroxyl at the adjacent phosphorus atom [36]. Inhibition of cleavage at higher concentrations of imidazole can be attributed to competition of positively charged imidazole molecules (at pH 7.0 half of imidazole is protonated and thus positively charged) and Dp12 for the binding with negatively charged RNA internucleotide phosphates.

As shown in Fig. 6, cleavage of ON21 by Dp12 is considerably affected by buffer type (Tris–HCl, HEPES–KOH, MES–KOH, NaAc–HAc, potassium cacodylate–KOH or KH_2PO_4). For comparison, the highest activity of Dp12 was taken as 100%. The reaction is entirely suppressed in the phosphate buffer. Apparently, inactivation of Dp12 in phosphate buffer results from the competition between phosphate ions and internucleotide phosphates of RNA for binding with Dp12 molecules. This result clearly shows that electrostatic interactions between positively charged DABCO residues and negatively charged internucleotide phosphate groups are essential for cleavage. In general, cleavage extent depends on the buffer type: in buffers HEPES, MES and Tris, containing strong anions (sulfate or chloride), cleavage efficiency is higher, than in acetate or cacodylate buffers containing strong cations (sodium or potassium). Thus, strong cations at total concentration 250 mM (including cations concentration from buffer) inhibited Dp12/RNA interaction. It can be explained by competition of cations from buffer with positive charged Dp12 molecules for binding with negatively charged phosphates.

The influence of type and concentration of monovalent cations on RNA cleavage by Dp12 was assayed under standard conditions except for K^+ was replaced by Li^+, Na^+, Cs^+ or NH_4^+ and concentration of monovalent cations varied from 0 to 400 mM (Fig. 7). The patterns of ON21

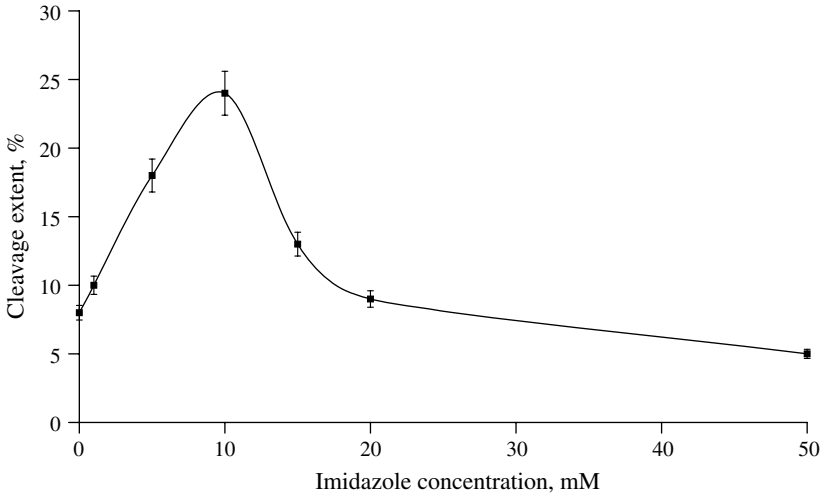

Fig. 5. Stimulation by imidazole of Dp12-catalyzed cleavage of [5′-^{32}P]-ON21. Reaction conditions: 5 μM ON21,10 μM Dp12, 50 mM Tris–HCl, pH 7.2, 0.2 M KCl, 0.1 mM EDTA, imidazole at concentration from 0 to 50 mM, 37 °C, 2 h.

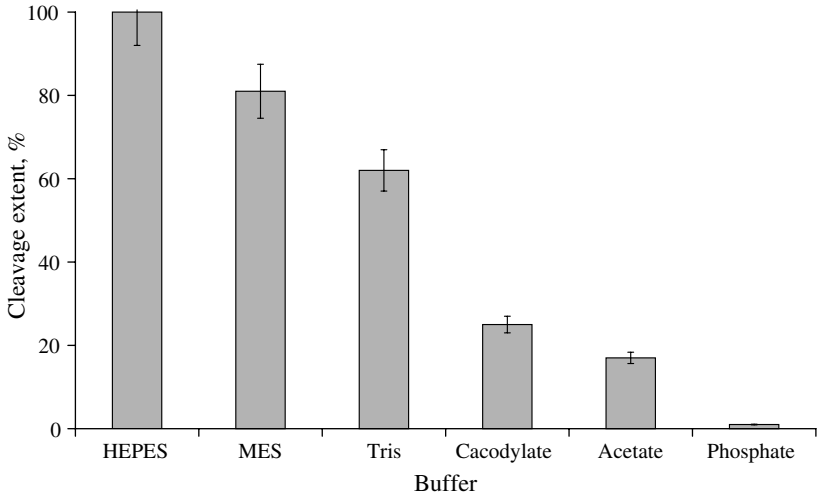

Fig. 6. Influence of buffer type on [5′-^{32}P]-ON21 cleavage by compound Dp12. Extent of ON21 cleavage in HEPES buffer is assumed to be 100%. Reaction conditions: 5 μM ON21, 10 μM Dp12, 50 mM buffer, 0.2 M KCl, 0.1 mM EDTA, 37 °C, 12 h.

cleavage by Dp12 in the presence of K^+ and other monovalent cations (see Fig. 7a for example) were similar. The main cleavages occurred at two adjacent C—A phophodiester bonds and at the highest activity conditions (see 100 mM of NH_4^+ in Fig. 7a) C_9—C_{10} bond within the loop was also cleaved. The data in Fig. 7b shows that efficiency of ON21 cleavage by Dp12 is strongly affected by cations size and concentration. Cleavage in the absence of monovalent cations occurs very slowly, and cleavage extent is increased with the increasing of monovalent cations concentration. The monovalent ions concentration profile is a bell-shaped curve with the maximum either at 100 mM or at 200 mM. In the presence of Li^+, Na^+, NH_4^+ maximal cleavage activity is observed at 100 mM concentration of cations and these rates are 2-fold lower then the ones observed in the presence of K^+ or Cs^+. In the presence of the latter cations, the maximal cleavage activity was higher (60–70% of ON21 was cleaved in 8 h at 37 °C) and observed at 0.2 M concentration.

4. Discussion

Cleavage of RNA can occur under mild conditions, due to the presence of 2′-hydroxyl group in the ribose residue of RNA, which makes possible the intramolecular nucleophylic attack at the adjacent phosphorus atom. This process can be accelerated by many factors including alkaline pH, where ionization of 2′-OH^- group can occur, and natural ribonucleases. It worth to note, that the most active aRNases enhance RNA cleavage at about 10^4–10^5 folds [33,37], while for natural ribonucleases 10^{12} rate acceleration is achieved.

Dp12 is aRNase built of two positively charged DABCO residues and two dodecamethylene fragments (Fig. 1). Four positive charges of two DABCO residues allow this conjugate to bind with negatively charged RNA molecules. As compared with aRNases investigated earlier [9,10], Dp12 does not contain functionalities known to catalyze of transesterification reaction. Surprisingly, this compound displays reasonable ribonuclease activity. Thus, it is interestingly to know why conjugate of cationic DABCO and lipophilic fragments do cleave RNA.

Interaction of RNA with Dp12 assayed by light scattering shows, that firstly, Dp12 displays the highest catalytic activity at concentration (10^{-5} M) far below the CMC, therefore the possibility of ‘‘micellar catalysts’’ occurring at the positively charged surface of micelles formed by Dp12 can be excluded. Secondly, by the static light scattering we found, that the interaction of Dp12 in optimal concentration with RNA substrates results in formation of large supramolecular complexes RNA/Dp12 (the complex size correlates with RNA length), cleavage of RNA occurs within these complexes and size of complex is gradually decreased in the course of RNA cleavage. Thirdly, it is likely, that at Dp12 concentrations over 10 μM, some multimeric Dp12 aggregates or micelles are formed (see Fig. 3a), which results in sharp decrease and even disappearance of Dp12 ribonuclease activity. Under these conditions, concentration of free monomolecular Dp12 become low and not sufficient to interact with RNA efficiently.

Analysis of specificity of RNA cleavage by Dp12 shed some light on the possible mechanism of this process. Fig. 8 displays sequence-specificity of RNA cleavage by Dp12 as number of phosphodiester bonds of a given type cleaved by Dp12 within tested RNAs in comparison with total number of these bonds present within these RNAs. It is seen, that U—A and C—A phosphodiester bonds, as expected, are more readily cleaved by Dp12 (cleavage of all U—A and C—A bonds is observed; both primary and secondary cuts are taken into account). Approximately a half of C—C, U—C, C—U, and C—G phosphodiester bonds present in the RNAs is cleaved. Therefore, relative rates of cleavage of different linkages in RNA by Dp12 are decreased in the order: CA, UA > CU, CC, CG >

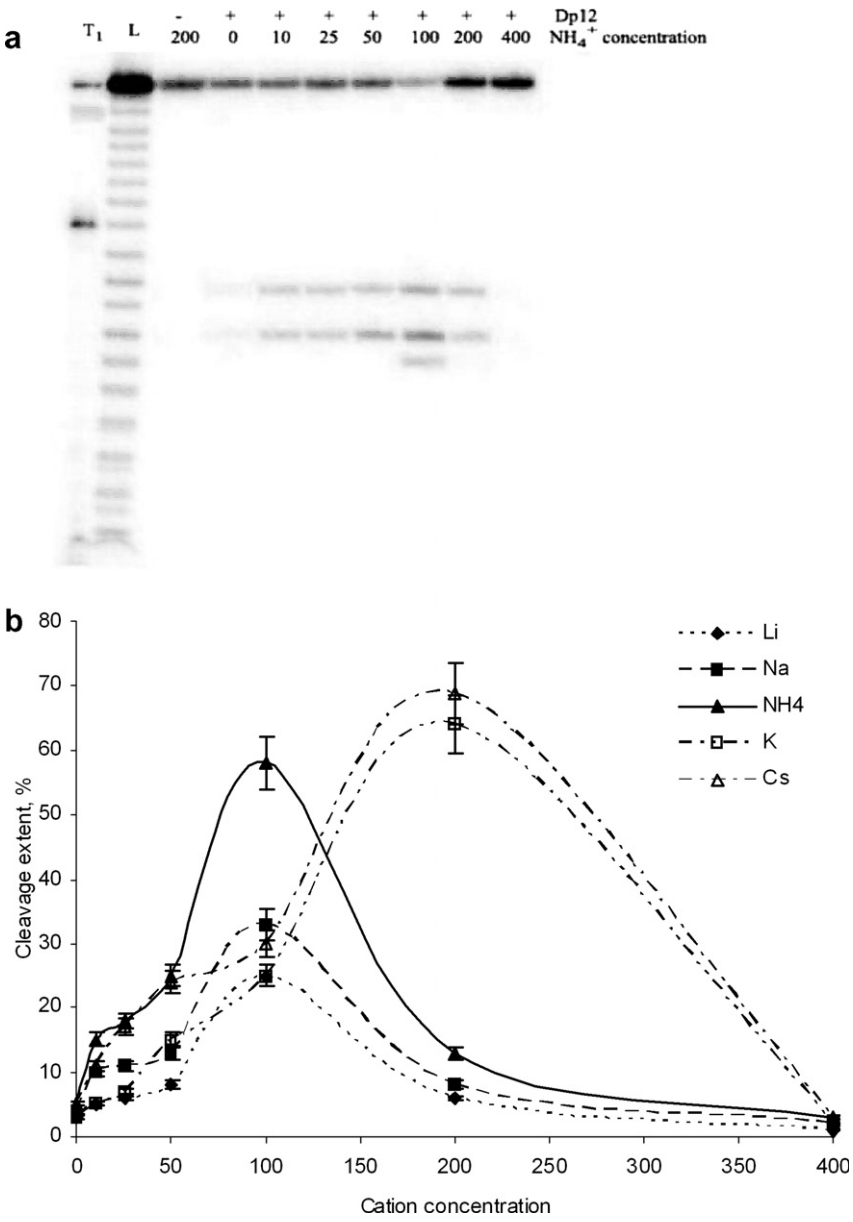

Fig. 7. Effect of cation concentration and type on cleavage of [5′-^{32}P]-ON21 with compound Dp12. (a) Cleavage of ON21 by Dp12 in the presence of NH_4^+. Autoradiograph of 15% denaturing PAAG. L and T1—partial hydrolysis of ON21 in 2 M imidazole buffer, pH 7.0 and by RNase T1 under denaturing conditions, respectively. (b) Quantitative data on cleavage of ON21 by Dp12 in the presence of different monovalent cations. Reaction conditions: 5 μM of ON21, 10 μM of Dp12, 50 mM Tris–HCl, pH 7.2, 0.1 mM EDTA, X^+ (Li^+, Na^+, K^+, Cs^+, or NH_4^+) at concentrations from 0 to 0.4 M, 37 °C, 12 h.

UC > UG, AG, GG. This specificity correlates well with the relative rates of spontaneous cleavage of different RNA linkages in water solution [38,39]. Generally, the ability of RNA linkages to self-cleavage can be placed in the following order: UA > CA > YC > YG > YU (Y = U or C) [38,39]. Therefore, one can assume that in Dp12/RNA multiplex Dp12 molecules interact with each internucleotide phosphate and sequence-specificity of RNA cleavage is determined by the mutual stability of each phosphodiester bond. However, the main question which remains to be answered is how Dp12 enhances rate of RNA self-cleavage?

Four alternative ways to accelerate internal phosphodiester transfer involving 2′-hydroxyl group in RNA summarized in [40] are the following: (1) in-line conformation fitness; (2) neutralization of negative charge on a nonbridging phosphate oxygen; (3) deprotonation of the 2′-OH group; (4) neutralization of negative charge on the 5′-oxygen atom. It seems likely, that Dp12, similar to ribozymes and deoxyribozymes, can catalyze transesterification reaction using ways (1) and (3).

Conformation changes in RNA backbone followed Dp12 binding could be firstly due to direct RNA internucleotide phosphates' conformation bending and secondly

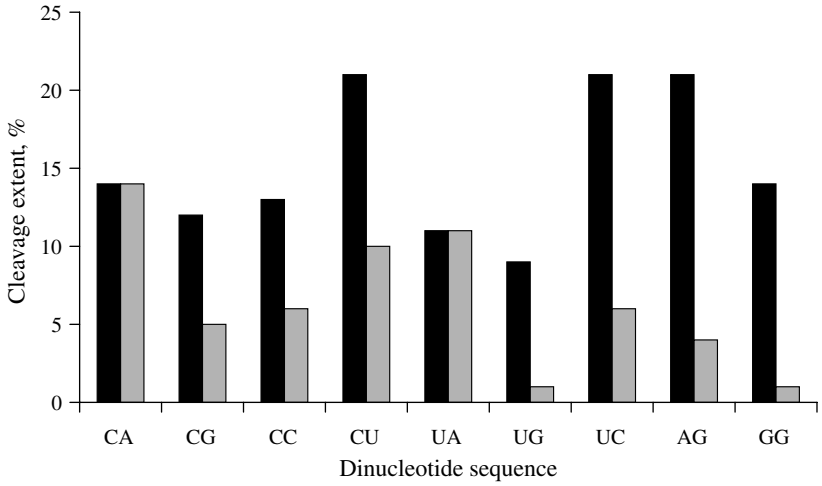

Fig. 8. Sequence-specificity of RNA cleavage by Dp12. The diagram displays total numbers of different dinucleotide sequences in all tested RNA substrates (ON21, yeast $tRNA^{Phe}$, HIV1 RNA, MDR RNA) (black bars) and the number of particular phosphodiester bonds, cleaved within these substrates by Dp12 (grey bars). Non-cleaved linkages are not shown at the diagram.

due to water-mediated conformation bending. Direct RNA backbone bending is possible upon multiplexes RNA/Dp12 formation: Dp12 molecules form with RNA particles with hydrophobic interior and RNA molecules at the positively charged outer side (Fig. 9a). In these multiplexes, conformation of internucleotide phosphates might be altered and could adopt an "in-line" geometry (Fig. 9b).

The second way is changing of water surrounding of ribose-phosphate backbone in the presence of Dp12. As shown in [41, 42], water surrounding influence is crucial for conformation of nucleic acids: for example, when water surrounding is restricted by some factors (e.g., different cations), DNA changes B conformation to A due to changes in the conformation of the sugar residues. In the hydratation layer of molecules of ionic detergents the ratio of bound to free water was found to be 9:1 [43], so water is structured in this interface. It was shown, that structured water is essential for catalysis of RNA cleavage by ribozymes [44, 45]. Therefore, upon interaction with RNA, Dp12, containing hydrophilic "head" and hydrophobic "tale", can affect microenvironment of phosphodiester bonds and as a result of this, change the conformation of riboso-phosphate backbone, which is crucial for self-cleavage.

The obtained data on the influence of monovalent cations on RNA cleavage by Dp12 (Figs. 6 and 7c) also confirm our hypothesis on the important role of bound and free water in the RNA cleavage. In the absence of monovalent cations, polyanionic RNA assumes a rod like conformation due to repulsion of the phosphates, therefore attack of 2′-hydroxyanion at internucleotide phosphate needed for transesterification can hardly occur. In the presence of moderate concentrations of monovalent ions the RNA charges are neutralized and RNA can easily assume different conformations.

According to [46–48] monovalent ions can be divided into two groups: chaotrops and cosmotrops depending on the

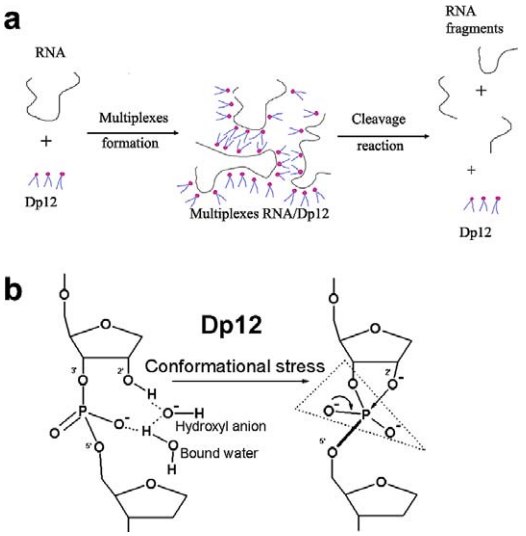

Fig. 9. Tentative mechanism of RNA cleavage by compound Dp12. (a) Dp12 and RNA in solution form multiplexes with average molecular weight over 100 MDa. (b) In these multiplexes conformational stress (1) and bound water (2) facilitate fitness of riboso-phosphate backbone to "in-line" conformation and access of OH^--groups to cleaved linkage (3).

ability for binding and structuring water molecules around them. Cosmotropic cations have large affinity to cosmotropic anions, and similarly to chaotropic ions. Thus, in our case cosmotrops Li^+, Na^+ strongly bind to cosmotropic internucleotide phosphates and interfere with the cationic chaotrop Dp12. This explains relatively small increase of cleavage activity of Dp12 in the presence of Li^+, Na^+ and lower (100 mM) concentration of ions at which maximum stimulation is observed. Binding of chaotropic cations (K^+, Cs^+) to the RNA phosphates is weak and these cations compete with Dp12 for the phosphates less efficiently. At higher concentrations (cosmotrops at lower, chaotrops at higher concentration) all monovalent cations prevent Dp12 from binding to RNA and inhibit the cleavage reaction.

Therefore, obtained results are consistent with our suggestion that ribose-phosphate backbone conformation bending (conformational stress) can be the main reason for efficient RNA cleavage in the presence of Dp12. Recently, conformational effect has been invoked to understand catalytic strategies in various systems [40, 49–52], including enzymes [49–52] and ribozymes [40]. Average rate enhancement due to conformational effect for RNA intramolecular transesterification reaction was found [40, 53] to be about 12–20-fold and the maximum rate enhancement is probably could not exceed 10^2 [40]. These data correlate well with the obtained results on cleavage rate enhancement at different pH observed in the presence of Dp12: 12–90-fold (Fig. 4a). It is likely that total rate enhancement achieved in Dp12-catalyzed reaction is much higher: k_{obs} measured 10 mM Dp12 is 4×10^{-6} s^{-1}, while k_{obs} for self-cleavage measured under similar conditions is about 100 times lower. However, we can not calculate directly total rate enhancement, because the order of catalyzed reaction is higher then first in respect to catalyst. We can only assume that rate acceleration of RNA cleavage by Dp12 in comparison to RNA self-cleavage is several orders of magnitude.

The conformational effect is possibly not the only factor providing RNA-cleavage rate enhancement by Dp12. One of the possibilities is that Dp12 accelerate transesterification reaction in RNA (Fig. 9b) by shielding negative charges of internucleotide phosphate by the bound positively charged 1,4 diazabicyclo [2.2.2] octane and facilitating access of OH^- groups from solution to the 2′-OH group. The obtained pH profiles are in accordance with this possibility: dependence of log k_{obs} versus pH is almost linear especially for pH interval 5.8–8.0 with the slope 0.24, whereas similar dependence for self-cleavage has the slope 0.44 (Fig. 4b). These results correlate well with pH profile expected for RNA self-cleavage [40] where linear part of the curve corresponding to pH interval 5.5–13.5 has the slope +1. The differences between experimental data (0.44) and predicted data (1.0) for RNA self-cleavage can be explained by the influence of the particular sequence and structure of RNA substrate used in the experiments (ON21). Effect of RNA context, nearest neighbor and structure on sensitivity of phosphodiester bonds cleavage are well documented. Nevertheless, slopes for catalytic and non-catalytic reactions obtained in the parallel experiments differ by factor 2. This means that influence of OH^- concentration is higher for non-catalytic cleavage. Apparently, Dp12 facilitates access of OH^--groups to RNA and the rate enhancement caused by increasing of the concentration of hydroxyl-ions is not so significant. From the other hand, this result can also be explained by the formation of some RNA-catalyst multiplexes.

5. Conclusions

Dp12, lacking functionalities known as catalysts of transesterification reaction efficiently catalyzes phosphodiester bonds cleavage. The compound functionally mimics ribonucleases—possesses catalytic and binding subsites, forms multiplexes with RNA molecules and bend phosphodiester bonds to achieve "in-line" conformation, thus facilitating transesterification. This conformational bending probably occurs due to the change of water surrounding phosphodiester bonds after binding with Dp12. Hydrophobic part of Dp12 molecule disturbs water surrounding and plays a role of a catalytic subsite of Dp12 molecule.

Acknowledgments

This work was supported by Grants RFBR 05-04-48985, RFBR 04-04-48566, FCSTP RI-112/001/254, RAS programs "Molecular and cellular biology", "Science to medicine", "Origin of life and evolution of the biosphere". Authors are grateful to Dr. M.G. Semenova for help in carrying out light scattering measurements, Ms. E. Burakova for synthesis of Dp12.

References

[1] N. Kovalev, E. Burakova, V. Silnikov, M. Zenkova, V. Vlassov, Bioorg. Chem. 34 (2006) 274–286.
[2] M. Yashiro, R. Kawahara, J. Biol. Inorg. Chem. 9 (2004) 914–921.
[3] M. Hertweck, M.W. Mueller, Eur. J. Biochem. 268 (2001) 4610–4620.
[4] S. Kazakov, S. Altman, Proc. Natl. Acad. Sci. USA 88 (1991) 9193–9197.
[5] R. Haener, J. Hall, G. Rihs, Helv. Chem. Acta 80 (1997) 487–494.
[6] M. Komiyama, J. Sumaoka, Curr. Opin. Chem. Biol. 2 (1998) 751–757.
[7] J. Ciesiolka, in: J. Barciszewski, B.F.C. Clark (Eds.), RNA Biochemistry and Biotechnology, Kluwer, Dordrecht, 1999, pp. 111–121.
[8] M. Brannvall, N.E. Mikkelsen, L.A. Kirsebom, Nucleic Acids Res. 29 (2001) 1426–1432.
[9] R. Giege, B. Felden, M.A. Zenkova, V.N. Sil'nikov, V.V. Vlassov, Methods Enzymol. 318 (2000) 147–165.
[10] D.A. Konevetz, I.E. Beck, N.G. Beloglazova, I.V. Sulimenkov, V.N. Sil'nikov, M.A. Zenkova, G.V. Shishkin, V.V. Vlassov, Tetrahedron 55 (1999) 503–514.
[11] A. Bibillo, M. Figlerowicz, R. Kierzek, Nucleic Acids Res. 27 (1999) 3931–3937.
[12] R. Kierzek, Methods Enzymol. 341 (2001) 657–675.
[13] M.A. Podyminogin, V.V. Vlassov, R. Giege, Nucleic Acid Res. 21 (1993) 5950–5956.
[14] M. Zenkova, N. Beloglazova, V. Sil'nikov, V. Vlassov, R. Giege, Methods Enzymol. 341 (2001) 468–490.
[15] M.A. Zenkova, A.V. Vlassov, D.A. Konevetz, V.N. Sil'nikov, R. Giege, V.V. Vlassov, Bioorg. Chem. (Moscow) 26 (2000) 610–616.
[16] V.N. Silnikov, N.P. Lukyanchuk, G.V. Shishkin, R. Giege, V.V. Vlassov, Dokl. Acad. Nauk 360 (1998) 554–558.
[17] N.G. Beloglazova, V.N. Silnikov, M.A. Zenkova, V.V. Vlassov, FEBS Lett. 481 (2000) 277.
[18] N.G. Beloglazova, M.M. Fabani, M.A. Zenkova, E.V. Bichenkova, N.N. Polushin, V.V. Sil'nikov, K.T. Douglas, V.V. Vlassov, Nucleic Acids Res. 32 (2004) 3887–3897.
[19] M.A. Zenkova, N.G. Beloglazova, in: M. Zenkova (Ed.), Artificial Nucleases, Nucleic Acids and Molecular Biology, vol. 13, Springer-Verlag, 2004, pp. 189–221.
[20] K. Valegard, J.B. Murray, P.G. Stockley, N.J. Stonehouse, L. Liljas, Nature 371 (1994) 623–626.
[21] D. Scherly, W. Boelens, N.A. Dathan, W.J. van Venrooij, I.W. Mattaj, Nature 345 (1990) 502–506.
[22] W.F. Lima, H. Wu, J.G. Nichols, T.P. Prakash, V. Ravikumar, S.T. Crooke, J. Biol. Chem. 278 (2003) 49860–49867.

[23] T. Hakoshima, M. Tanaka, T. Itoh, K.I. Tomita, T. Amisaki, S. Nishikawa, H. Morioka, S. Uesugi, E. Ohtsuka, M. Ikehara, Protein Eng. 4 (1991) 793–799.
[24] S. Niranjanakumari, T. Stams, S.M. Crary, D.W. Christianson, C.A. Fierke, Proc. Natl. Acad. Sci. USA 95 (1998) 15212–15217.
[25] R.T. Raines, Chem. Rev. 3 (1983) 1045–1065.
[26] T.E. England, O.C. Uhlenbeck, Biochemistry 17 (1978) 2069.
[27] J.M. Evans, in: M.B. Huglin (Ed.), Light Scattering from Polymer Solutions, Academic Press, London, 1972, pp. 89–164.
[28] C. Tanford, Physical Chemistry of Macromolecules, Wiley, New York, 1961.
[29] W. Burchard, in: S.B. Ross-Murphy (Ed.), Physical Techniques for the Study of Food Biopolymers, Blackie, Glasgow, 1994, pp. 151–214.
[30] D.S. Horne, in: E. Dickinson (Ed.), New Physico-Chemical Techniques for the Characterization of Complex Food Systems, Blackie, Glasgow, 1995, pp. 240–267.
[31] L.G. Tyulkina, A.S. Mankin, Anal. Biochem. 138 (1984) 285–290.
[32] P. Romby, D. Moras, P. Dumas, J.-P. Ebel, R.J. Giege, Mol. Biol. 195 (1987) 193–204.
[33] R. Ting, J.M. Thomas, L. Lermer, D.M. Perrin, Nucleic Acids Res. 29 (2004) 6660–6672.
[34] E.V. Kostenko, R.S. Beabealashvilly, V.V. Vlassov, M.A. Zenkova, FEBS Lett. 475 (2000) 181–186.
[35] V.V. Vlassov, G. Zuber, B. Felden, J.P. Behr, R. Giegé, Nucleic Acids Res. 23 (1995) 3161–3167.
[36] P. Jarvanen, M. Oivanen, H. Lonnberg, J. Org. Chem. 56 (1991) 5396–5401.
[37] N.L. Mironova, D.V. Pyshnyi, D.V. Shtadler, A.A. Fedorova, V.V. Vlassov, M.A. Zenkova, Nucleic Acids Res. 35 (2007) 2356–2367.
[38] R. Kierzek, Nucleic Acids Res. 20 (1992) 5073–5077.
[39] R. Kierzek, Nucleic Acids Res. 20 (1992) 5079–5084.
[40] G.M. Emilsson, S. Nakamura, A. Roth, R. Breaker, RNA 9 (2003) 907–918.
[41] W. Saenger, Ann. Rev. Biophys. Biophys. Chem. 16 (1987) 93–114.
[42] J. Barciszewski, J. Jurczak, S. Porowski, T. Specht, V.A. Erdmann, Eur. J. Biochem. 260 (1999) 293–307.
[43] S. Balasubramanian, S. Pal, B. Bagchi, Curr. Sci. 84 (2003) 428–430.
[44] M.M. Rhodes, K. Reblova, J. Sponer, N.G. Walter, Proc. Natl. Acad. Sci. USA 103 (2006) 13380–13385.
[45] M.V. Krasovska, J. Sefcikova, K. Reblova, B. Schneider, N.G. Walter, J. Sponer, Biophys. J. 91 (2006) 626–638.
[46] K.D. Collins, Proc. Natl. Acad. Sci. USA 92 (1995) 5553–5557.
[47] K.D. Collins, Biophys. J. 72 (1997) 65–76.
[48] Y.V. Kalyuzhnyi, V. Vlachy, K.A. Dill, Acta Chim. Slov. 48 (2001) 309–316.
[49] T.C. Bruice, Chem. Rev. 8 (2006) 3119–3139.
[50] J.L. Gao, K.L. Byun, P. Kluger, Top. Curr. Chem. 238 (2004) 113–136.
[51] H. Guo, Q. Cui, W.N. Lipscomb, M. Karplus, Proc. Natl. Acad. Sci. USA 98 (2001) 9032–9037.
[52] K.E. Ranaghan, A.J. Mulholland, Chem. Commun. 10 (2004) 1238–1239.
[53] D. Min, S. Xue, H. Li, W. Yang, Nucleic Acids Res. 35 (2007) 4001–4006.